

# Interaction of matter-wave gap solitons in optical lattices

Beata J. Dąbrowska, Elena A. Ostrovskaya  
and Yuri S. Kivshar<sup>§</sup>

Nonlinear Physics Centre and Australian Centre for Quantum-Atom Optics, Research School of Physical Sciences and Engineering, Canberra ACT 0200, Australia

**Abstract.** We study mobility and interaction of gap solitons in a Bose-Einstein condensate (BEC) confined by an optical lattice potential. Such localized wavepackets can exist only in the gaps of the matter-wave band-gap spectrum and their interaction properties are shown to serve as a measure of discreteness imposed onto a BEC by the lattice potential. We show that inelastic collisions of two weakly localized near-the-band-edge gap solitons provide simple and effective means for generating strongly localized in-gap solitons through soliton fusion.

Submitted to: *J. Opt. B: Quantum Semiclass. Opt.*

<sup>§</sup> Corresponding author. E-mail address: ysk124@rsphysse.anu.edu.au (Yuri Kivshar)

## 1. Introduction

Periodic potentials created by optical lattices are by now recognized as a powerful tool for controlling and manipulating nonlinear matter waves through dynamical diffraction management [1, 2]. One of the important implications of such management is creation of nonlinearly localized matter-wave packets, the so-called *bright atomic solitons*, in a Bose-Einstein condensate with a positive scattering length, i.e. with *repulsive* inter-atomic interaction. Such a counter-intuitive effect can occur as wave localization in the gaps of the band-gap spectrum due to the Bragg scattering of coherent matter waves by the periodic potential of an optical lattice [4]. Since the repulsive atomic interactions prohibit a collapse of the bright wavepackets and the solitonic nature of their evolution ensures fixed spatial phase variations due to mean-field effects, the atomic gap solitons may represent an attractive high-density source for atomic interferometry [3].

The possibility of nonlinear localization in a repulsive BEC was established theoretically [4, 5, 6, 7], being recently confirmed experimentally in the case of one-dimensional optical lattices [8]. The experimental challenge of the gap soliton generation and manipulation is two-fold. First, the BEC wavepacket, initially loaded into a ground (Bloch) state of the optical lattice potential, should be accelerated to the edge of the first Brillouin zone. The regime of the wavepacket preparation and the dynamical transition to the band edge dramatically affects the outcome of the experiment [10], and in the best case scenario only weakly localized low-atom-number gap solitons near the bottom edge of the spectral gap can be generated using the current experimental techniques [8]. The depth of the gap, where the gap solitons contain large atom numbers and are well localized [6] is yet to be accessed. Secondly, the possibility of the gap soliton manipulation, which is essential for interferometric applications, can be limited by impaired mobility of the gap solitons due to effects of lattice discreteness [11].

In this paper, we examine the problem of mobility and interactions of gap solitons in a one-dimensional optical lattice without an additional harmonic confinement, within the framework of the continuous Gross-Pitaevskii model with a periodic potential. We show that, as the chemical potential of a BEC scans the spectral gap, the gap solitons display a variety of scattering properties ranging from those of “ideal” solitons without a periodic potential to those of nonlinear localized excitations of discrete nonlinear lattices [12]. In addition, we suggest that the inelastic collisions of near-the-band-edge gap solitons can provide reliable means for generating highly-localized high-density immobile atomic solitons in the depth of the spectral gap.

## 2. Model

We consider the dynamics of a cigar-shape BEC cloud in the presence of a one-dimensional optical lattice. In dimensionless units the Gross-Pitaevskii (GP) equation

governing the evolution of the condensate wavefunction can be written as:

$$i\frac{\partial\psi}{\partial t} = \left( -\frac{1}{2}\frac{\partial^2}{\partial x^2} + V(x) + \sigma|\psi|^2 \right) \psi, \quad (1)$$

where the optical lattice potential  $V(x) = V_0\sin^2(\pi x/d)$  is uniform and characterized by its depth  $V_0$  measured in units of lattice recoil energy  $E_r = \hbar^2\pi^2/(2md^2)$ , and lattice period  $d$ . The condensate wave function is normalized to:  $\int_{-\infty}^{+\infty} dx|\psi(x,t)|^2 = Ng_{1D}$ , where  $N$  is the number of atoms,  $g_{1D} = 2|a_s|/a_0$ ,  $a_s$  is the s-wave scattering length, and  $a_0$  the characteristic harmonic oscillator length in the direction of tight confinement. For  $^{87}\text{Rb}$  atoms with  $m = 1.44 \times 10^{-25}\text{kg}$ ,  $a_s = 5.3\text{nm}$  and assuming a transverse frequency  $\omega_{\perp} \sim 2\pi \times 10^2\text{Hz}$ , gives  $g_{1D} \sim 10^{-2}$ . The coefficient  $\sigma = \text{sgn}(a_s) = \pm 1$  characterizes the type of the atomic interactions. In what follows we consider repulsive interaction, i.e.  $\sigma = 1$ , and set  $d = 1$ , which corresponds to  $\approx 1.1 \mu\text{m}$  lattice spacing.

Stationary states of a condensate are described by solutions of Eq.(1) of the form:  $\psi(x;t) = \phi(x)\exp(-i\mu t)$ , where the steady-state wave function  $\phi(x)$  obeys the *time-independent* GP equation

$$\left( -\frac{1}{2}\frac{d^2}{dx^2} + V(x) + \sigma|\phi|^2 \right) \phi = \mu\phi. \quad (2)$$

In the case of a noninteracting condensate ( $\sigma = 0$ ) stationary solutions of equation (2) are Bloch waves,  $\phi(x) \sim b(x,k)\exp(ikx)$ , where  $b(x)$  have periodicity of the lattice and  $k$  is the quasi-momentum. The linear spectrum  $\mu(k)$  of the Bloch states has a characteristic band-gap structure, with the lowest two bands shown in figure 1(a) in the parameter plane  $(V_0, \mu)$ . The shaded areas correspond to the regions where oscillating solutions of equation (2) (Bloch waves) exist. The clear areas correspond to the spectral gaps which appear due to the Bragg scattering of the matter waves in a periodic structure, being the forbidden domains for matter wave propagation. The gap below the first band is the trivial semi-infinite "total internal reflection" gap. The first finite gap is where the formation of gap solitons in repulsive BEC occurs [6, 7]. The condition  $\mu = V_0$  roughly delineates between the regimes of tight-binding ( $\mu < V_0$ ) and superfluid ( $\mu > V_0$ ) behavior. In what follows, we investigate the dynamics of gap solitons in the lattice of height  $V_0 = 10$  which places the first gap into a relatively tight-binding regime.

The nonlinear localization of a BEC with positive scattering length ( $\sigma = +1$ ) in the first spectral gap has been well studied both theoretically [6, 7] and experimentally [8]. The stationary localized solutions of equation (2) - gap solitons - can be found at any value of  $\mu$  inside the spectral gap. The number of atoms contained in a localized state is small near the lowest gap edge and raises as the chemical potential moves inside the gap [6]. The lowest-order families of *on-site* (OS) and *inter-site* (IS) gap solitons, centered on the lattice minimum or maximum, respectively, are shown in figure 1(b). The characteristic "staggered" spatial structure of both OS and IS solitons can be seen in figure 1(c).

### 3. Mobility of gap solitons

In order to study interactions of gap solitons, one has to generate mobile localized states. It has been shown, however, that the mobility of a matter wave soliton in an optical lattice is restricted by the existence of the so-called Peierls Nabarro (PN) potential barrier [11, 12]. The concept of the PN barrier originates from the theory of dislocations and later studies of mobility of localized nonlinear excitations in discrete lattices [13, 14]. The PN barrier is introduced as the height of the effective periodic potential generated by the lattice discreteness, and it defines the minimum energy required to move the centre of mass of a localized wavepacket by one lattice site [13]. Extending this definition to the continuous lattice model, one can define the PN barrier as the energy difference between the on-site and inter-site localized stationary states [11]. Since the OS and IS states can be mapped to represent a moving mode at different times, the PN barrier can be calculated as the smallest amount of energy that a gap soliton needs to gain in order to start moving along the lattice. Even in the tight-binding regime, the amount of the energy needed to initiate the soliton motion is not in agreement with the estimate of the PN barrier height derived from the corresponding discrete nonlinear Schrödinger model [11], therefore the use of the continuous model in the study of gap soliton motion and interactions is well justified.

A soliton solution of equation (2) is characterized by its dynamical invariants: number of atoms and energy. The soliton energy can be calculated as:

$$E = \int dx \left[ -\frac{1}{2} \phi^* \frac{d^2}{dx^2} \phi + V(x) |\phi|^2 + \frac{1}{2} \sigma |\phi|^4 \right]. \quad (3)$$

The on-site (OS) gap soliton is a localized state with the lowest energy, and therefore it is this state that is eventually generated from an arbitrary initial wavepacket. The PN potential height associated with this state is given by  $U_{PN} = E_{IS} - E_{OS}$ . The threshold value of the momentum (per atom) that a soliton must have to overcome the barrier is defined as  $k_{PN} = (2U_{PN}/N)^{1/2}$ . Such a momentum can be applied experimentally either by ultrashort laser pulses or a tilt of the optical lattice potential imposed by a gravitational field or by a slope of a harmonic trap. The PN potential per atom calculated for the family of OS gap solitons within the first gap is shown in figure 2(a). In contrast, the inter-site state corresponds to a maximum of the PN potential and is *unstable against small perturbations* of its center-of-mass position. Such perturbation will lead to conversion of the IS soliton into an OS soliton, as shown in figure 3.

To investigate the dynamics of the OS gap soliton with a finite velocity, we solve the evolution equation (1) numerically. The initial condition is given by  $\psi(x; t = 0) = \phi_0(x) \exp(-ik_0x)$ , where  $\phi_0$  is a stationary gap soliton wavefunction, and  $k_0$  is an initial momentum per atom. The values of  $k_0$  were chosen below, above, or at the threshold value  $k_{PN}$ . The results of the calculations are shown in figure 2(b,c,d). Due to the large negative group-velocity dispersion [16], solitons near the edge of the lower band exhibit *anomalous steering*, i.e. initially the direction of motion is opposite to the momentum kick received. Oscillating motion within a single lattice site has

been observed for an initial  $k_0$  values below and at the threshold [see figure 2(b,c)]. Above the threshold kinetic energy (which is still an order of magnitude lower than an individual lattice well depth) a soliton undergoes free motion across the lattice, as shown in figure 2(d). During this motion, an atomic soliton evolves through many states centered on different points of the optical lattice. Periodic revival of the states closely resembling the stationary states of the IS and OS families [figure 1(c)] can be observed, however due to a loss of atoms neither number of atoms contained in a soliton nor  $\mu$  are conserved during the evolution. The loss of atoms from the moving localized state increases with growing  $k_0$ .

The mobility properties of gap solitons vary depending on their chemical potential. Close to the lowest gap edge ( $\mu < 7.5$  in our case), gap solitons are well described by the effective nonlinear Schrödinger equation (NLS) for the slowly varying envelope of a Bloch state [9]. In this regime, solitons are expected to behave like lattice-free envelope solitons of the integrable NLS model. Indeed, they exhibit free motion for arbitrary small initial momentum due to very small energy difference between the OS and IS stationary solutions of equation (2). These states are weakly localized and contain only about 100 atoms. Deeper in the gap ( $7.5 < \mu < 8.2$ ), the mobility properties of solitons are similar to those of localized solutions of the discrete NLS equation, and can be very well described by the concept of the PN barrier. In the regime where the solitons are strongly localized in the vicinity of a single lattice well ( $\mu > 8.2$ ), their dynamics is dominated by oscillations of the centre of mass within a single lattice site for moderate initial perturbations. The soliton motion with a large initial velocity is accompanied by significant loss of atoms from the localized structure.

#### 4. Binary collisions of gap solitons

Depending on the value of the chemical potential and degree of localization, gap solitons display a variety of scattering properties. In particular, we study binary collisions of in-phase solitons numerically for a range of values of the chemical potentials near the bottom edge of the gap, which is the experimentally accessible region of soliton generation [8]. We keep the initial separation of soliton centers the same in all cases and chose the same initial velocity above the PN threshold. Similar interaction conditions can be realized by imposing an additional harmonic confinement onto the system.

Three regimes of soliton collisions have been identified in our simulations. The first one is the regime where in-phase solitons ( $\Delta\phi = 0$ ) interact elastically, i.e. without momentum and energy exchange [see figure 4 (a)]. In this narrow parameter domain ( $7.3 < \mu < 7.35$ ) the dynamics of the gap solitons resembles the dynamics of "ideal" solitons of the completely integrable NLS equation without the lattice potential. The total momentum of the system is defined as:

$$P = i \int dx \left( \frac{d\psi^*}{dx} \psi - \psi^* \frac{d\psi}{dx} \right), \quad (4)$$

and its zero value before and after collision indicates that the soliton collisions are not affected by the lattice periodicity.

Deeper in the gap the solitons start to experience stronger localization and their dynamics become inelastic. Significant radiation usually accompanies the collisions, and the total momentum of the system is no longer conserved. This is the typical signature of a discrete system [12], and a consequence of nonintegrability introduced by a periodic potential. The effect of small perturbations (numerical noise which emulates noise in the real physical system) accounts for the spontaneous symmetry breaking (SB) and generation of finite momentum during the collision process [12]. In this “weakly discrete” regime of the soliton dynamics, the solitons can exhibit multiple collisions [12]. In the multiple collisions solitons “bounce” from each other leading to either final separation or fusion, see figure 4(b,c). For  $\mu \geq 7.43$  the solitons merge into a single localized state, as seen in figure 4(d), which due to SB moves in an unpredictable direction across the lattice and exhibits large amplitude oscillations. The appearance of SB, multiple collisions and the total momentum generation has been observed for a range of the chemical potential  $7.35 < \mu < 7.5$ .

For our choice of the optical lattice depth, the solitons relatively close to the lower gap edge (e.g. for  $\mu = 7.5$ ) already exhibit strongly inelastic scattering behavior characteristic of a discrete system. For the values of the chemical potential  $\mu \geq 7.5$  the binary collisions lead to fusion of two solitons into a single localized state. Unlike the outcome of fusion after multiple collisions, the resulting solitons move with nearly zero velocity and damped amplitude oscillations, as can be seen in figure 5. Location of the initial states (containing around 170 atoms each) on the branches of stationary solutions, is indicated by point A in figure 1(b). After collision, an immobile highly-localized soliton containing a larger number of atoms is generated. From the  $N$  vs.  $\mu$  dependence [see figure 1(b)] it can be inferred that the generated soliton, consisting of approximately 270 atoms, lies deeper in the gap than the initial states [see point B in figure 1(b)]. Therefore, inelastic collision of weakly localized near-the-gap-edge solitons can, in principle, be employed for a formation of fundamental atomic gap solitons with a larger number of atoms in the depth of the spectral gap, i.e. in the region of parameters that is currently inaccessible experimentally. This technique can be useful for any number of colliding solitons near the band edge. In particular, the case of triple-soliton collisions is illustrated in figure 6, where the phase of the central soliton was inverted by  $\pi$  to achieve soliton merging.

For solitons located even deeper in the gap, the binary collisions inevitably result in their fusion, and the emerging localized states remain confined within a single lattice well, although their centre of mass can oscillate around the potential minimum. The amplitude of the centre of mass oscillations increases with  $\mu$ , however the value of the total momentum averaged over the time  $\Delta t$  at  $\sim 20$  oscillations:  $\langle p \rangle = \frac{1}{\Delta t} \int_{t_0}^{t_0+\Delta t} p dt$ , remains close to zero. The values of the post-collision velocity of the localized state (relative to the initial velocity  $v_0$ ) and the average momentum vs. chemical potential of the colliding solitons in the vicinity of the gap edge are plotted in figure 7. It can

be clearly seen that the initial stage of quasi-elastic collisions ( $\langle p \rangle \approx 0$ ,  $v = v_0$ ) and final stage of the soliton fusion ( $\langle p \rangle \approx 0$ ,  $v \approx 0$ ) is separated by the symmetry breaking stage, where the outcome of collisions is not predictable. We note that the symmetry breaking outcome of soliton collisions is also characteristic of binary collisions of solitons with non-zero phase difference, as in the case of a localized state in the discrete NLS model [12].

## 5. Conclusions

We have studied numerically both mobility and interaction of the matter-wave gap solitons in an experimentally accessible regime, i.e. near the lowest edge of the spectral gap of an optical lattice. For the collision velocities above the Peierls-Nabarro mobility threshold, the gap solitons demonstrate scattering dynamics scenarios ranging from quasi-elastic collisions to soliton fusion. By employing the inelastic collision of two or three gap solitons in configurations that can be realized experimentally, for instance, in a combination of an optical lattice and a harmonic trap, we showed that the soliton fusion can be successfully used to generate stationary matter-wave solitons deep in the spectral gap. Applying the same technique to solitons with different amplitudes can potentially enable generation and steering of a mobile high-density soliton. Such a process of gap-soliton manipulation may eventually lead to new possibilities for the preparation of sources for atomic interferometry [3].

## Acknowledgement

This work was partially supported by the Australian Research Council (ARC). The Australian Centre for Quantum-Atom Optics is an ARC Centre of Excellence.

## References

- [1] Eiermann B, Treutlein P, Anker Th, Albiez M, Taglieber M, Marzlin K P and Oberthaler M K 2003 *Phys. Rev. Lett.* **91** 060402
- [2] Fallani L, Cataliotti F S, Catani J, Fort C, Modugno M, Zawada M and Inguscio M 2003 *Phys. Rev. Lett.* **91** 240405
- [3] Pötting S, Zobay O, Meystre P and Wright E M 2000 *J. Mod. Opt.* **47** 2653
- [4] Zobay O, Pötting S, Meystre P and Wright E M 1999 *Phys. Rev. A* **59** 643
- [5] Konotop V V and Salerno M 2002 *Phys. Rev. A* **65** 021602
- [6] Louis P J, Ostrovskaya E A, Savage C M and Kivshar Yu S 2003 *Phys. Rev. A* **67** 013602
- [7] Efremidis N K and Christodoulides D N 2003 *Phys. Rev. A* **67** 063608
- [8] Eiermann B, Anker Th, Albiez M, Taglieber M, Treutlein P, Marzlin K P and Oberthaler M K 2004 *Phys. Rev. Lett.* **92** 230401
- [9] see, e.g., Steel M J and Zhang W 1998 *Preprint cond-mat/9810284*
- [10] Anker Th, Albiez M, Eiermann B, Taglieber M and Oberthaler M K 2004 *Opt. Express* **11** 681
- [11] Ahufinger V, Sanpera A, Pendri P, Santos L and Lewenstein M 2004 *Phys. Rev. A* **69** 053604
- [12] Papacharalampous I E, Kevrekidis P G, Malomed B A and Frantzeskakis D J 2003 *Phys. Rev. E* **68** 046604

- [13] Kivshar Y S and Campbell D K 1993 *Phys. Rev. E* **48** 3077
- [14] Braun O M and Kivshar Yu S 2004 *The Frankel-Kontorova Model, Concepts, Methods and Applications* (Berlin: Springer) p 31
- [15] Semagin D A, Dmitriev S V, Sheigenari T, Kivshar Yu S and Sukhorukov A A 2002 *Phys. B* **317-318** 136-138
- [16] Neshev D, Sukhorukov A A, Hanna B, Królikowski W and Kivshar Yu S 2003 *Preprint* nlin.PS/0311059



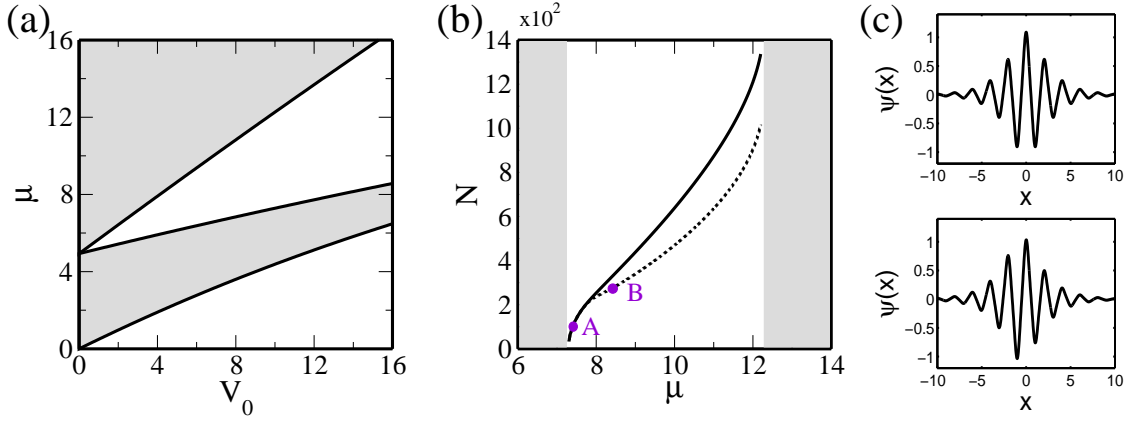


**Figure 1.** (a) Band-gap structure of the matter-wave spectrum  $\mu(V_0)$ . (b) Families of the on-site (OS, dotted) and inter-site (IS, solid) gap solitons for  $V_0 = 10.0$ , within the first gap. Point A (B) corresponds to the location of an initial (final) state in figure 6. (c) Spatial profiles of the OS (top) and IS (bottom) gap solitons at  $\mu = 7.5$ .

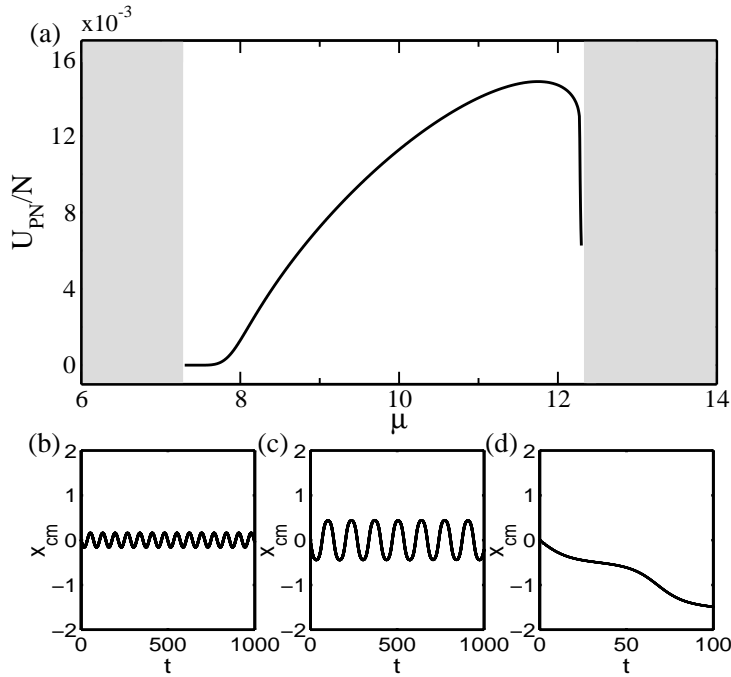


**Figure 2.** Top: (a) PN potential for gap solitons presented in figure 1(b) as a function of  $\mu$  within the first gap. Bottom: Examples of soliton centres of mass dynamics for  $\mu = 7.7$  with the PN threshold momentum  $k_{PN} = 1.20 \times 10^{-2}$  and the initial momentum (b) below the PN threshold,  $k_0 = 6.01 \times 10^{-3}$ , (c) near the threshold  $k_0 = 1.20 \times 10^{-2}$ , and (d) above the threshold  $k_0 = 1.24 \times 10^{-2}$ .

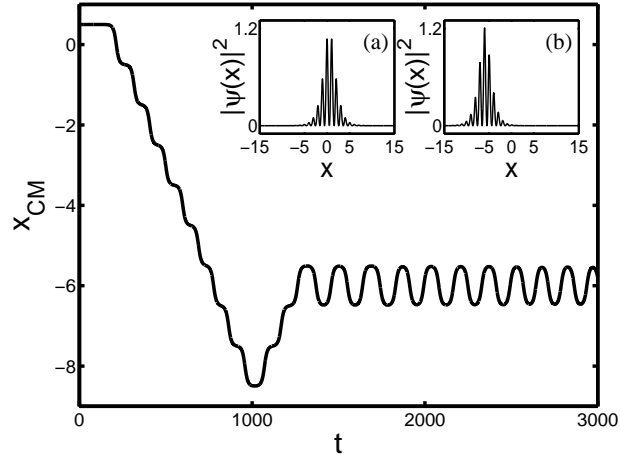


**Figure 3.** Evolution of the centre of mass of the initially stationary IS gap soliton at  $\mu = 7.7$ . Insets: (a) Initial spatial profile, and (b) spatial profile at the time  $t = 3 \times 10^3$ , showing the characteristic structure of the OS state.

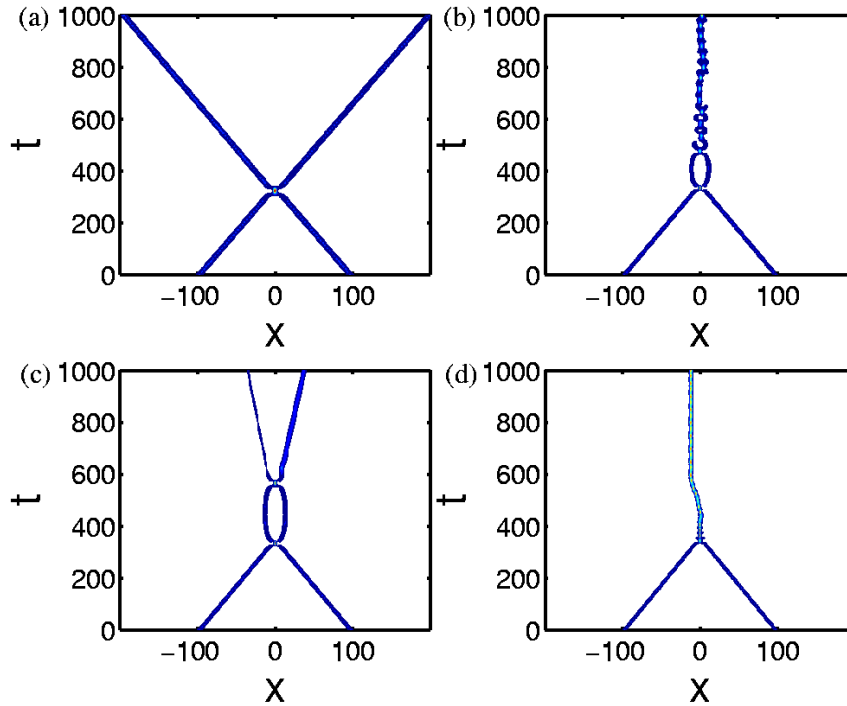


**Figure 4.** Examples of soliton interactions in the nonintegrable NLS regime for different values of the chemical potential (a)  $\mu = 7.35$ ; (b)  $\mu = 7.405$ ; (c)  $\mu = 7.41$ ; (d)  $\mu = 7.45$  and  $k_0 = 0.1$ .

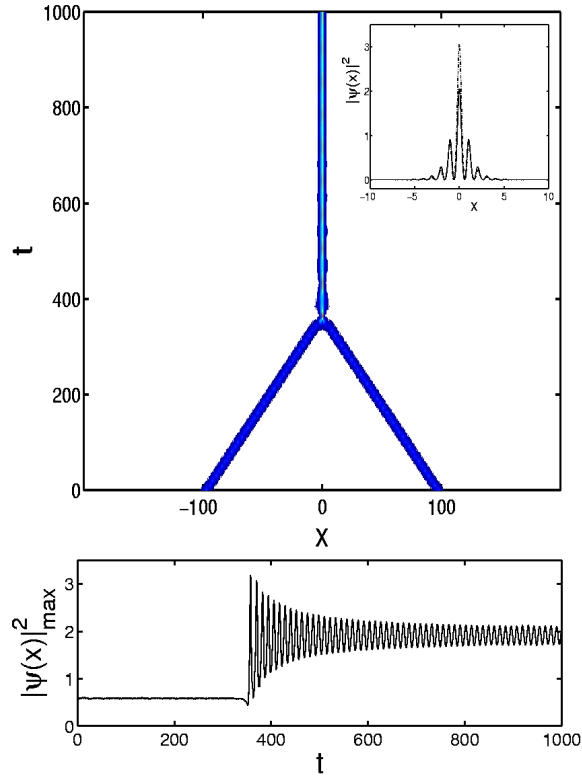


**Figure 5.** *Top: Typical scenario of soliton fusion with zero final velocity in the discrete NLS regime ( $\mu = 7.5$ ) Initial momentum of the soliton pair  $|k_0| = 0.1$ .; Inset: Solid - typical spatial profile of the post-collision trapped state at  $t = 10^3$ , dashed - exact OS solution corresponding to point B in figure 1(b),  $\mu = 8.36$ . Below: Evolution of the peak density of the trapped state showing transition to a trapped highly-localized in-gap state corresponding to the marked point B in figure 1(b).*

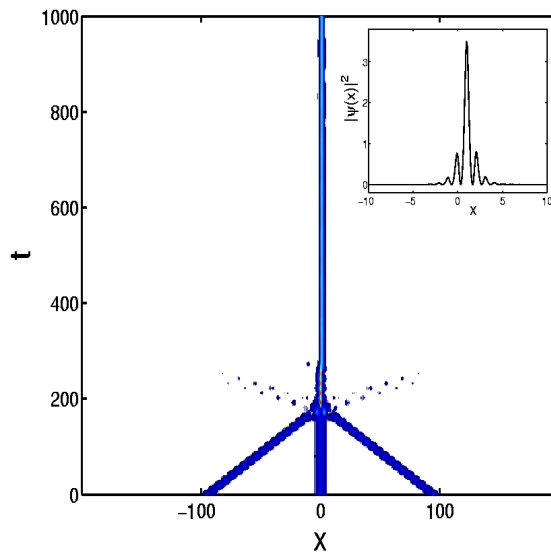


**Figure 6.** *Typical scenario of triple-soliton fusion in the discrete NLS regime ( $\mu = 7.5$ ), with the central immobile soliton  $\pi$ -out of phase with the others. Initial momentum of the off-centre soliton pair  $|k_0| = 0.2$ .; Inset: typical spatial profile of the post-collision trapped state at  $t = 10^3$ .*

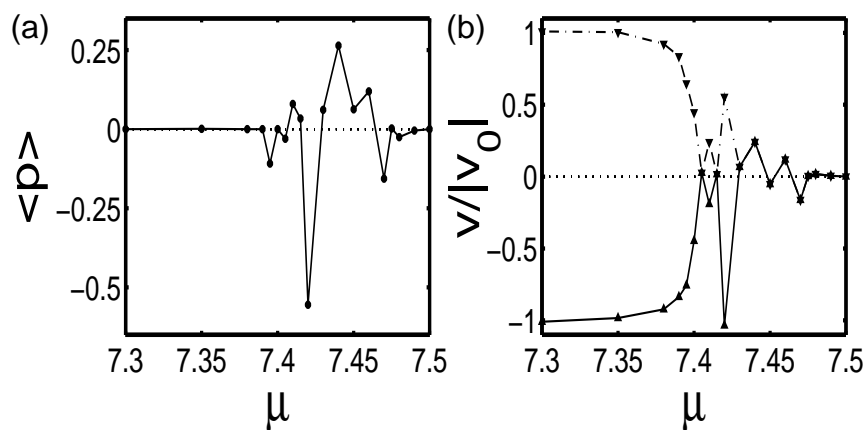


**Figure 7.** Post-collision (at  $t = 10^3$ ) (a) time-averaged momentum of gap solitons as a function of  $\mu$  within the first gap and (b) relative velocity of the soliton pairs. Behavior characteristic for  $k_0 = 0.1$ .